RB-33

# EFFECT OF MAGNETIC DEFLECTION ON ELECTRON BEAM CONVERGENCE

RADIO CORPORATION OF AMERICA
RCA LABORATORIES
INDUSTRY SERVICE LABORATORY

RADIO CORPORATION OF AMERICA

RCA LABORATORIES

INDUSTRY SERVICE LABORATORY

# RB-33

# Effect of Magnetic Deflection on Electron Beam Convergence

# Effect of Magnetic Deflection on Electron Beam Convergence

The image curvatures of deflection yokes are calculated and minimized using third order perturbation theory. It is found that the mean image curvature is too large to dispense with dynamic convergence when a point focus is needed. Proper field shaping, however, can produce a good line focus over the whole screen without dynamic convergence.

## Introduction

The quality of deflection yokes has become increasingly important. Larger screens call for larger deflection angles and color kinescopes have three beam guns, which implies a much larger convergence angle than a single beam. The misconvergence of yokes is proportional to both the deflection angle and the convergence angle. In consequence, it has been necessary to introduce "dynamic convergence" as a means of keeping the three beams converged over the whole surface of the screen. Since the dynamic convergence requirement increases the cost of guns as well as circuitry and also introduces an effect known as "degrouping", it is important to minimize or eliminate the need of dynamic convergence by minimizing or eliminating those aberrations of the deflection yoke which are responsible for misconvergence.

This bulletin investigates the aberrations of a deflection coil, using its symmetry properties, by a perturbation treatment developed by W. Glaser and G. Wendt[1,2]. It will be shown that significant improvement over present yokes is possible for line-screen kinescopes and that the length of the yoke field is the most important parameter.

## Description of the Magnetic Field

Magnetic deflection fields as they are used in television tubes have as a common property the symmetry group to which they belong. If we take as the z-axis the axis of the tube and the x and y axes as the horizontal and vertical axes, then the symmetry property of a *vertical deflection* yoke coil (Fig. 1) is given by:

$$\begin{aligned} H_x(x,y,z) &= H_x(-x,y,z) = H_x(x,-y,z) \\ H_y(x,y,z) &= -H_y(-x,y,z) = -H_y(x,-y,z) \\ H_z(x,y,z) &= -H_z(-x,y,z) = H_z(x,-y,z) \end{aligned} \tag{1}$$

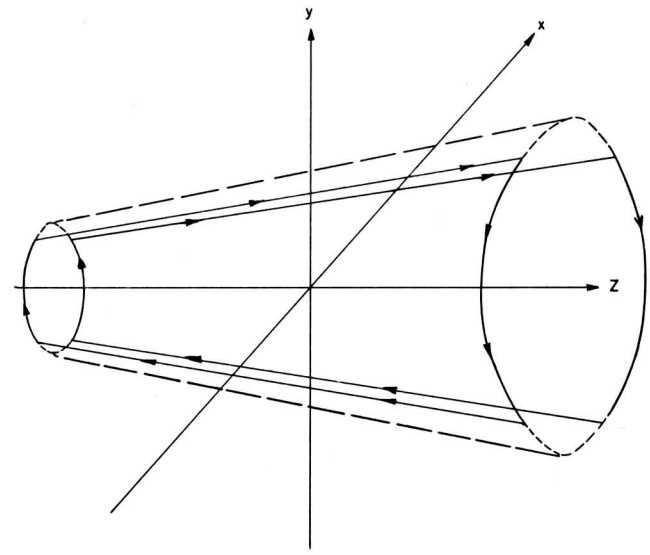


Fig. 1. Symmetry of a vertical deflection coil.

In the region of deflection, the field has to obey Maxwell's equations for a region free of charge, current or electric field:

$$\begin{aligned} \text{curl } \vec{H} &= 0 \\ \text{div } \vec{H} &= 0 \end{aligned} \tag{2}$$

Equations (1) and (2) limit the possibilities of choices for deflection fields considerably. In a power series expansion of the field one obtains:

$$H_x = H_1(z) - \left[H_2(z) + H_1''(z)/2\right] x^2 + H_2(z)y^2 + \text{fourth order terms}$$

1. W. Glaser, *Z. Physik*, III, 357 (1938).

2. G. Wendt, *Telefunkenrohre*, No. 15, 100 (1938).

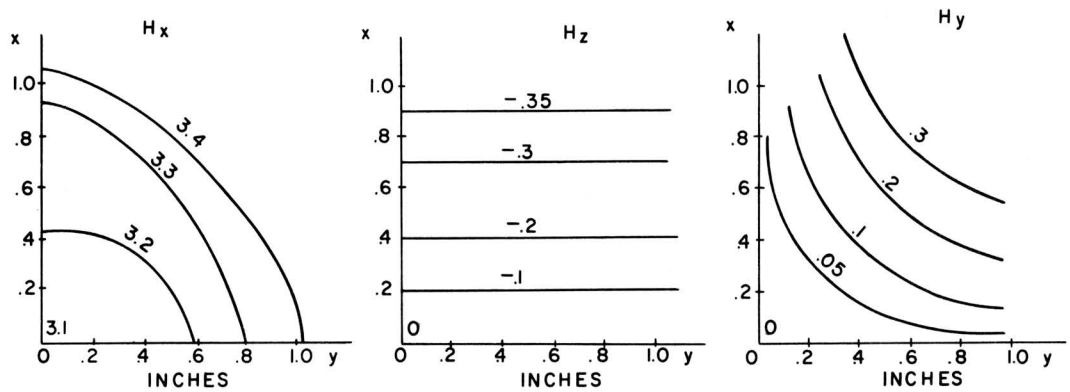


Fig. 2. Lines of constant field strength.

$$H_y = 2H_2(z)xy + \text{fourth order terms} \qquad (3)$$

$$H_z = H_1'(z)x + H_2'(z)xy^2 - \frac{1}{6}\left[H_1''(z) + 2H_2'(z)\right]x^3 + \text{fourth order terms}$$

where $H'(z) = dH(z)/dz$.

The meaning of (3) is that for sufficiently small x and y, the curves for $H_x$ = constant are ellipses or hyperbolae in a plane z = constant. The curves $H_y$ = constant are hyperbolae. The curves $H_z$ = constant are slightly more complicated, but for very small x and y they are straight lines parallel to the y-axis.

Fig. 2 gives a plot of $H_x$, $H_y$, and $H_z$ as it was measured in a typical deflection yoke at some arbitrary z = constant. Of course, equations (3) need no experimental verification, being a simple consequence of the symmetry properties of the yoke coils and Maxwell's equation. The figures do indicate, however, for what ranges of x and y a third order expansion of the field will give good approximation.

Equations (3) also show that the whole field in the region where third order theory is good, is given by two arbitrary functions $H_1(z)$ and $H_2(z)$. Therefore, in order to know the field, it is only necessary to obtain these functions. This is easily done by measuring the total field along two lines parallel to the z-axis: (a) The z-axis itself (x = 0, y = 0,) (b) Some line of constant y and x = 0 ($x = 0, y = y_c$). (a) Will give $H_1(z)$ directly as can be seen by an inspection of (3). (b) Will give $H_1(z) + H_2(z)y_c^2$.

This means that simply measuring the total field at say ten points on line (a) and line (b) makes it possible to pass tenth-order ploynomials through $H_1(z)$ and $H_2(z)$, which in turn specify the whole field in the regions of interest.

The third order expansion should be good for deflection angles of up to 25 degrees. This is perfectly adequate for questions of convergence, since certain boundary conditions about the surfaces of best convergence will then make it possible to extrapolate to any desired deflection angle, as will be demonstrated later.

Now introduce a vector-potential $\vec{A}$, such that

$$\vec{H} = \text{curl } \vec{A}$$

One particular choice of $\vec{A}$ is the following:

$$A_x = 0 + \text{fourth order terms}$$

$$A_y = (1/2)H_1'(z)x^2 + \text{fourth order terms} \qquad (4)$$

$$A_z = H_1(z)y + (1/3)H_2(z)y^3 - H_2(z)x^2y + \text{fifth order terms.}$$

## The Perturbation Method

### *Lagrangian and Equations of Motion*

The integration of the path by the perturbation method has been derived in detail for magnetic deflection fields[1][2]. Only as much of the argument will be repeated here as is necessary for an understanding of the conclusions.

The lagrangian for an electron trajectory can be written

$$W = \int_{P_o}^{P_1} F\,dz$$

in close analogy to Fermat's principle in light optics, where:

$$F = \eta\, ds/dz.$$

In electron optics, the index of refraction becomes:

$$\eta = (\zeta)^{1/2} - (e/2m)^{1/2} \left[A_x (dx/ds) + A_y (dy/ds) + A_z (dz/ds)\right]$$

$$\text{and } F = (\zeta)^{1/2} (1 + x'^2 + y'^2)^{1/2} - (e/2m)^{1/2} (A_x x' + A_y y' + A_z)$$

The function $\zeta$ is simply the electric potential taken with respect to a particle at rest and in the case of a purely magnetic field it is:

$$\zeta = mv^2/2e \qquad \text{, with } v^2 = \text{constant.}$$

Therefore:

$$G = F/\zeta^{1/2} = (1 + x'^2 + y'^2)^{1/2} - \mu(A_x x' + A_y y' + A_z) \quad (6)$$

with: $\mu = e/mv$

and $x' = dx/dz$

$y' = dy/dz$

Fermat's principle now states that the trajectory makes the lagrangian an extremum:

$$\delta \int_{z_o}^{z_1} G dz = 0 \qquad \delta G(z_1) = \delta G(z_o) = 0 \quad (7)$$

This leads to the Euler-Lagrange equations:

$$\begin{aligned} \partial G/\partial x - (d/dz)(\partial G/\partial x') &= 0 \\ \partial G/\partial y - (d/dz)(\partial G/\partial y') &= 0 \end{aligned} \quad (8)$$

substituting for G from (6) and then for the components of the vector potential from (4) gives the differential equations for the trajectories up to the third order:

$$\begin{aligned} &(d/dz)(x' - x'^3/2 - x'y'^2/2) \\ &\quad = -\mu\,[H_1'(z)xy' - 2H_2(z)xy\,] \\ &(d/dz)(y' - y'^3/2 - y'x'^2/2) \\ &\quad = -\mu\,[H_1(z) - H_2(z)x^2 - H_1''(z)x^2/2 \\ &\quad + H_2(z)y^2 - H_1'(z)xx'\,] \end{aligned} \quad (9)$$

The method of the perturbation calculation consists in solving the equations (9) for the terms which are first order in x, y, x', and y'. Then substitute the solutions for these quantities into the terms of higher order and solve the equations with the third order terms included. This solves the equations of motion up to terms of third order.

*The First Order Solution*

The equations (9) become after omission of the second and third order terms:

$$\begin{aligned} x'' &= 0 \\ y'' &= -\mu H_1(z) \end{aligned} \quad (10)$$

The asymmetry between x and y derives, of course, from the fact that the deflection field is for vertical deflection. Assuming the field to start at z = 0 and end at z = $l$, a restriction which will be discussed in detail later:

$$\begin{aligned} x &= x_o + zx_o' \\ y &= y_o + zy_o' - \mu \int_o^z dw \int_o^w H_1(v)dv \end{aligned} \quad (11)$$

Now, consider only rays which before deflection were going toward a point on the z-axis, say z = L, where L > $l$, (Fig. 3), and which at z = 0 were located at a radius r from the z-axis. In that case, introducing cylindrical coordinates,

$$\begin{aligned} x_o &= -r\cos\zeta & x_o' &= (r/L)\cos\zeta \\ y_o &= -r\sin\zeta & y_o' &= (r/L)\sin\zeta. \end{aligned} \quad (12)$$

Furthermore, define the convergence angle $\alpha$ as

$$(r/L) = \tan\alpha \approx \alpha.$$

Now assume, without loss of generality, that all terms of order $\alpha^2$ can be neglected. These terms do, in fact, introduce a deflection error known as "Koma"; however, the "Koma" does not affect the shape of the surfaces of best convergence. It does affect the quality of convergence, since it always broadens the spot.

The first order solution for a cone of rays originating on a circle of radius r at z = 0 and heading, before deflection, toward a point x = 0, y = 0, z = L, is:

$$\begin{aligned} x &= (z-L)\,\alpha\cos\zeta \\ y &= (z-L)\,\alpha\cos\zeta + D(z) \end{aligned} \quad (13)$$

where D(z) will be called the deflection:

$$D(z) = -\mu \int_o^z dw \int_o^w H_1(v)dv$$

It is seen from (13) that for z = L, where the screen is located

$$x = 0$$
$$y = D(L) \qquad (14)$$

and D(z) is strictly proportional to $H_1(z)$. This situation is also referred to as "perfect gaussian deflection". The whole cone, regardless of convergence angle or deflection angle, comes to a point of convergence at y = D(L), and D(L) depends linearly on $H_1(z)$. Any deviation from (14) will be called a "deflection error".

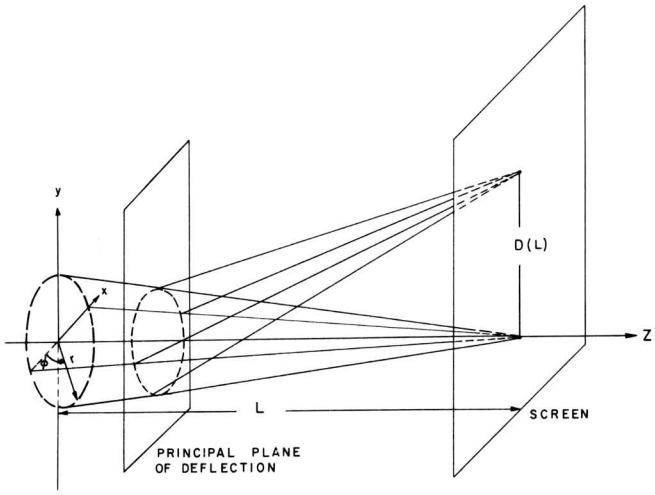


Fig. 3. Ideal deflection of a conical bundle.

*The Third Order Calculation*

The solution for the first order calculation is

$$x = (z\text{-}L)\alpha \cos \zeta$$
$$y = (z\text{-}L)\alpha \sin \zeta + D(z)$$
$$x' = \alpha \cos \zeta \qquad (15)$$
$$y' = \alpha \sin \zeta + D'(z)$$
$$\text{where: } D'(z) = -\mu \int_0^z H_1(w)\,dw$$

Substituting these values into equation (9) for the higher powers of x, y, x', and y', the equations can be easily integrated. Then write down the solutions for our original conical bundle of rays, and obtain for z = L, (neglecting terms of the order of $\alpha^2$):

$$x(L) = I_P \alpha \cos \zeta$$
$$y(L) = I_T \alpha \sin \zeta + D(L) + I_D. \qquad (16)$$

Here, $I_P$, $I_T$, and $I_D$ are integrals of the field quantities, which will be given later. They will be given the following names:

$I_P$ = Perpendicular astigmatism,

$I_T$ = Tangential astigmatism,

$I_D$ = Distortion.

Figs. 4, 5, and 6, will give these "errors" meaning. Fig. 4 is a picture in the x = 0 plane of the central ray (r = 0) and two rays whose original coordinates are given by: cos ζ = 0, sin ζ = ± 1. From (16), in that case

$$x(L) = 0$$
$$y(L) = \pm I_T \alpha + I_D + D(L).$$

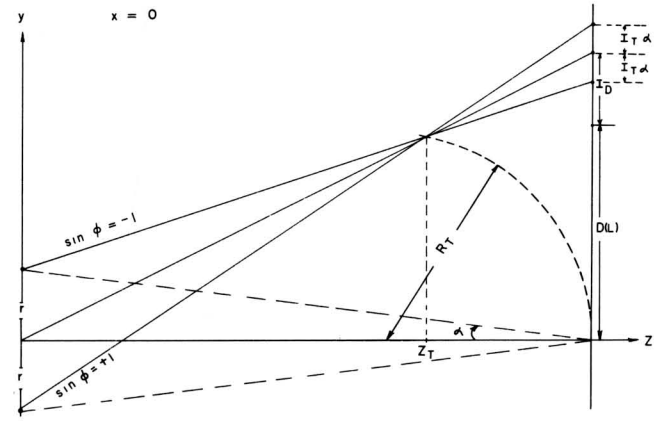


Fig. 4. Vertical deflection of tangential rays (sin φ equals ± 1).

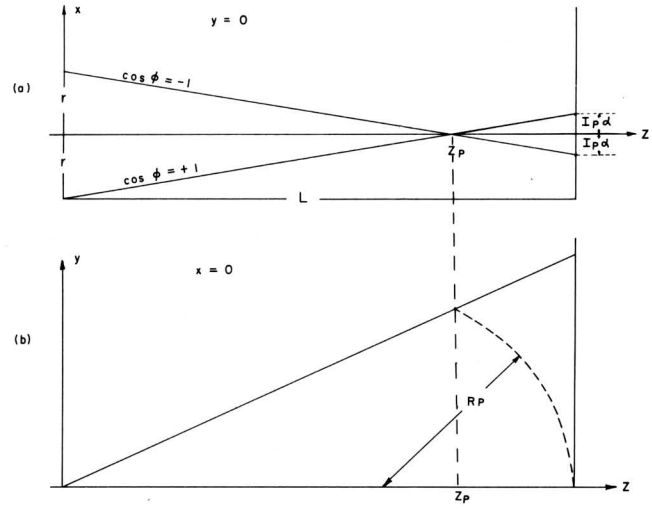


Fig. 5. Vertical deflection of perpendicular rays (cos φ equals ± 1).

For the central ray α = 0 and it will simply be displaced from the "perfect" position D(L) by an amount $I_D$. The rays coming from sin ζ = ± 1, will be displaced by an amount $\pm I_T \alpha + I_D$. If $I_T$ is positive (as it usually is), then the three rays will cross at a position $z = z_T$.

The curve which is generated by these crossings will be called the "Tangential Image Curvature" and its radius of curvature (constant in third order theory) is $R_T$.

Similarly, in Figs. 5a, and 5b, a projection of the rays characterized by initial position $\sin\theta = 0$, $\cos\theta = \pm 1$ are given in a plane y = constant and x = constant respectively. Here, the only distortion arises from the term $I_P$ and the two rays will cross at a position $z = z_P$. The curve which is generated by these crossings will be called the "Perpendicular Image Curvature" and its radius of curvature (constant in third order theory) is $R_P$.

Finally, there is a curve along which the whole bundle of rays form the smallest circle. It is along this curve that best overall convergence is obtained. This curve is called "Mean Image Curvature" and its radius of curvature R is given by:

$$(1/R) = (1/2)\left[(1/R_P) + (1/R_T)\right]. \qquad (17)$$

Fig. 6 gives a diagram of the total situation, showing the three image curvatures. In order to obtain good convergence, it is, therefore, desirable to maximize these radii of curvature, in order to make them correspond to the curvature of a screen that is not too severely curved towards the gun system. That the mean radius of convergence has definite upper limits will make up the main part of the rest of this bulletin.

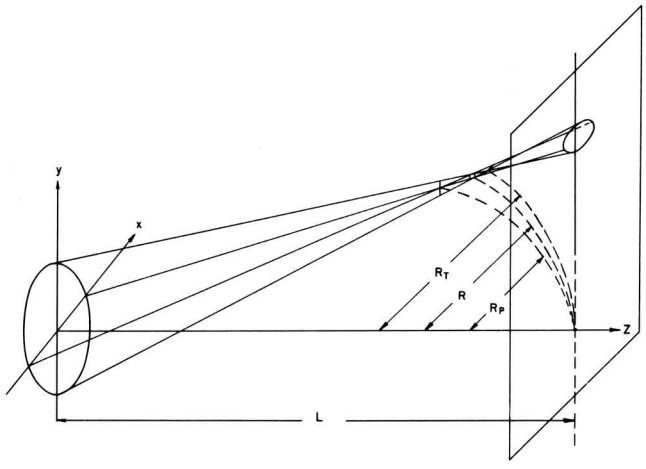


Fig. 6. The composition of astigmatism.

Let it also be mentioned, with respect to (16), that it thus appears that the ring of rays starting from z = 0, $x^2 + y^2 = r^2$, which has been considered, will on a flat screen at z = L, appear as an ellipse, whose center is at x = 0, $y = D(L) + I_D$ and whose axes are $I_P\alpha$ in the horizontal and $I_T\alpha$ in the vertical directions.

## The Surfaces of Convergence

In order to obtain the tangential, perpendicular, and mean image curvatures, i.e., $R_T$, $R_P$, and R, use is made of the fact that in third order theory these radii are constant. That means that without loss of generality the radii for infinitesimally small deviations can be calculated and they will hold for the whole region in which third order theory holds (up to deflection angles of about 25 degrees). Later, it will be shown how these can be extrapolated to higher angles.

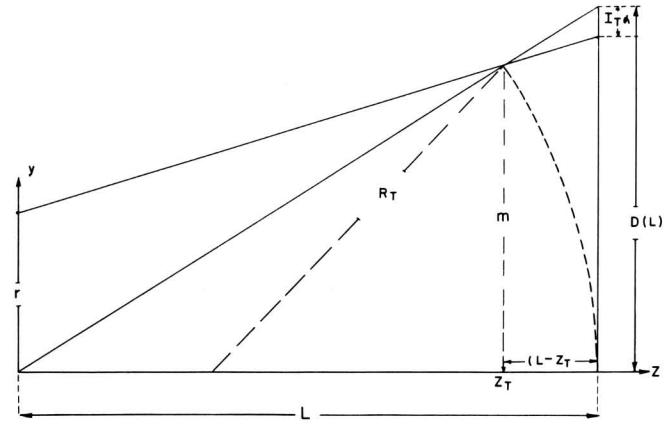


Fig. 7. Calculation of $R_T$.

For very small deviations, D can be considered as an infinitesimal quantity and quantities of the order of $D^2$ can be neglected. The calculation is made with reference to Fig. 7. Two relations hold exactly in that figure:

$$R_T^2 = m^2 + \left[R_T - (L-z_T)\right]^2 \qquad (18)$$

and

$$I_T\alpha/r = (L-z_T)/z_T. \qquad (19)$$

Consistent with the small angle of deviation, put

$$m^2 = D^2$$

and neglect $(L-z_T)^2$ compared to $(L-z_T)$. When these approximations are used consistently, (18) gives:

$$R_T = D^2/2\,(L-z_T);$$

and from (19), putting $\alpha z_T/r = z_T/L \approx 1$

$$R_T = D^2/2I_T. \qquad (20)$$

Similarly

$$R_P = D^2/2I_P; \qquad (21)$$

and from (17):

$$1/R = (I_T + I_P)/D^2. \tag{22}$$

Actually the quantities $I_T/D^2$ and $I_P/D^2$ will turn out to be independent of $D^2$ and it appears thus useful to define:

$$\begin{aligned} J_T &= I_T/D^2 \\ J_P &= I_P/D^2. \end{aligned} \tag{23}$$

Now:

$$\begin{aligned} 1/R_T &= 2J_T \\ 1/R_P &= 2J_P \\ 1/R &= J_T + J_P. \end{aligned} \tag{24}$$

Now give attention to the form of $J_T$ and $J_P$ and see their dependence on the field distribution $H_1(z)$ and $H_2(z)$. Assume that a conical bundle of rays enters the deflection field at $z = 0$. The deflection field is different from zero up to $z = l$. The original bundle was convergent on the z-axis at $z = L$. The aberrations $J_T$ and $J_P$ are then given by:

$$\begin{aligned} J_T &= (3/2)S_1 + 2S_2 \\ J_P &= -(1/2)S_1 - 2S_2 + S_3, \end{aligned} \tag{25}$$

where

$$\begin{aligned} S_1 &= \left[1/D(L)\right]^2 \int_0^L \left[D'(z)\right]^2 dz \\ S_2 &= \mu \left[1/D(L)\right]^2 \int_0^l H_2(z) D(z) (z-L)^2 dz \\ S_3 &= \mu^2 \left[1/D(L)\right]^2 \int_0^l H_1^2(z)(z-L)^2 dz. \end{aligned} \tag{26}$$

It will be remembered from (14) and (15) that:

$$D(z) = -\mu \int_0^z dw \int_0^w H_1(v)\,dv$$

and

$$D'(z) = -\mu \int_0^z H_1(w)\,dw.$$

It follows that:

$$D(L) = -\mu \int_0^l dz \int_0^z H_1(v)dv + (L-l)D'(l) \tag{27}$$

Substituting (25), (26) and (27) into the expression for (24),

$$1/R = \frac{\int_0^L \left[D'(z)\right]^2 dz + \mu^2 \int_0^l H_1^2(z)(z-L)^2 dz.}{D^2(L)} \tag{28}$$

The first important result is that (28) does not depend on $H_2(z)$ at all. This means that even though $R_T$ and $R_P$ depend very sensitively on $H_2(z)$, *the radius of best overall convergence depends only on the field along the axis, $H_1(z)$.* Secondly, it is obvious from (28) that 1/R and, therefore, R is always positive. This means that *the surface of best convergence must always bend towards the source of the electrons.*

It now remains to minimize the expression for 1/R, (28), which will maximize R and, therefore, yield the best possible field distribution.

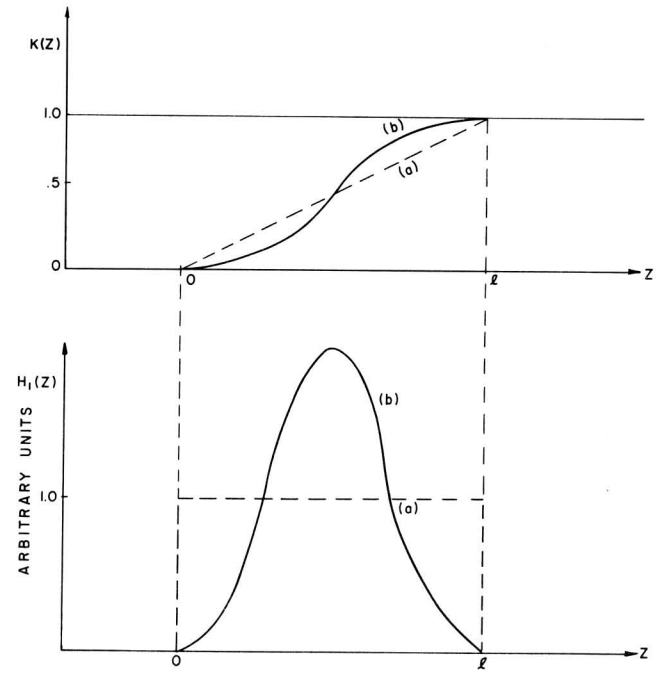


Fig. 8. Relationship between $K_{(Z)}$ and $H_{1(Z)}$.

In order to make (28) more amenable to mathematical treatment, introduce the following function:

$$K(z) = \left[\int_0^z H_1(w)\,dw\right] \Big/ \left[\int_0^l H_1(w)\,dw\right]. \tag{29}$$

In that case the reciprocal radius of image curvature becomes:

$$1/R = \left[\int_0^l K^2 dz + \int_0^l \dot{K}^2 (z-L)^2 dz + (L-l)\right] \Big/ \left[\int_0^l K dz + (L-l)\right]^2 \quad (30)$$

The boundary conditions on K(z) are:

$$\begin{aligned} K(0) &= 0 \\ K(l) &= 1 \\ \dot{K}(z) &= 0 \quad \text{for } z<0 \text{ and } z>l. \end{aligned} \quad (31)$$

The derivative of K(z) with respect to z, $\dot{K}(z)$, is simply $H_1(z)$ $\int_0^l H_1(z)dz$. The K(z) simply represents a normalized potential. Fig. 8 shows the relationship between K(z) and $H_1(z)$.

The next step is to minimize (30), which means finding that distribution of K(z) which will give a minimum 1/R. The results of this calculation will be given in the next section.

## Results

*The Uniform Field*

The solution of the equation

$$\delta(1/R) = 0$$

where (1/R) is given by (30), has proved to be too difficult in closed form. It was, therefore, desirable to use polynomials of a certain degree n, such as Legendre polynomials, for K(z), and minimize for each case. The first order case corresponds to a uniform field. This case is of particular interest, because it has been discussed by several authors in the past, mostly incorrectly, due to a disregard of Maxwell's equation. The first correct treatment and experimental verification of the uniform field case was given by Marschall and Schroder [3].

For the uniform field, K(z) takes the following form:

$$\begin{aligned} K(z) &= 0 \qquad z \leq 0 \\ K(z) &= z/l \qquad 0 \leq z \leq l \\ K(z) &= 1 \qquad l \leq z \end{aligned} \quad (32)$$

(See Fig. 8).

3. Marschall, H. and Schroder, E. Z. Tech. Phys. 23, 297, (1942). (The definition of L in that paper would correspond here to $L - (1/2)l$).

Substituting (32) in (30) we obtain:

$$(R/L) = (l/L)\left[1-(l/L) + (1/4)(l/L)^2\right] \Big/ \left[1 - (1/3)(l/L)^2\right] \quad (33)$$

To render this result dimensionless, we define new quantities:

$$\rho = R/L$$

$$\lambda = l/L.$$

Obviously $\lambda$ can vary from 0 to 1.

In terms of the parameters $\rho$ and $\lambda$, (33) becomes

$$\rho = \lambda\left[1-\lambda + (1/4)\lambda^2\right] \Big/ \left[1-(1/3)\lambda^2\right]. \quad (34)$$

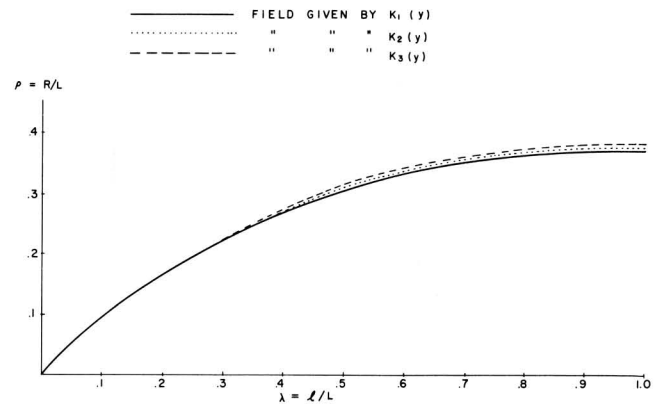


Fig. 9. Maximum radius of curvature for a polynomial expansion of the field.

The solid line in Fig. 9 gives a plot of equation (34). The main feature of this result is that for short fields ($l << L$ and, therefore, $\lambda << 1$) $\rho$ is equal to $\lambda$, and consequently:

$$R \approx l. \quad (35)$$

This means that for short yokes the image curvature is not related to the yoke to screen distance (L), as is widely believed, but is simply the length of the yoke field ($l$). As the length of the yoke field increases, i.e., as $\lambda$ approaches 1, the image curvature approaches

$$R \approx (3/8)L. \quad (36)$$

This result is in perfect agreement with Marschall and Schroder [3] and has been verified experimentally by them.

*Higher Order Solution*

The analysis of the uniform field still leaves the question open as to whether more general field distribu-

tions can yield a larger radius of curvature R, than is given by (33). For this purpose, higher order polynomials were used for K(z) and 1/R was minimized with respect to the parameters of the expansion. Of course, K(z) must obey its boundary conditions at z = 0 and z = $l$.

The expansion of K(z) was done in terms of Legendre Polynomials. In order to change the interval 0 to $l$ of z, into an interval -1 to +1, change variables from z to y, where y is given by

$$y = (2z/l) - 1. \tag{37}$$

Now more general expressions for K(z) can be given successively:

1st Order

$K_1(y) = (1/2)P_o(y) + (1/2)P_1(y)$ (Uniform field).

2nd Order

$K_2(y) = a_o P_o(y) + (1/2)P_1(y) + (1/2 - a_o)P_2(y)$.

3rd Order

$K_3(y) = a_o P_o(y) + a_1 P_1(y) + (1/2 - a_o)P_2(y) + (1/2 - a_1) P_3(y)$.

The minimum radii of curvature for each case are given in Fig. 9, in terms of $\rho$ = R/L and $\lambda$ = $l$/L.

The main result of this investigation is that the improvement that can be achieved by using a more general field distribution than the uniform field is completely insignificant. For example, always using the best choice of $a_o$ and $a_1$ in $K_3(y)$, we obtain:

$$\rho = \lambda(1 - \lambda + .13\lambda^2 + .06\lambda^3 + .01\lambda^4)/(1 - .52\lambda^2 - .01\lambda^3 + .04\lambda^4). \tag{38}$$

Quantitative comparison of (38) with (34), as shown in Fig. 9, demonstrates how insignificant the improvement of the more general third order field is over the uniform field.

*Equivalent Uniform Field*

For a practical application of the results in the preceding section, one point needs further clarification. Actual fields are not precisely confined to a region from 0 to $l$. In order to give the formulas meaning, therefore, we must define a length, which will be associated to an actual field distribution which ranges from plus to minus infinity. This is possible, particularly when one recognizes from (34) or (38) that R is sensitive to the length of the field only for short fields. Therefore, the formula for the equivalent length should be very good for short fields, $l < L/3$, and qualitatively correct for larger fields.

An analysis of (30) in connection with (29) and (34) gives for the effective $l$:

$$l_e = \left[\int_{-\infty}^{\infty} H_1(w)\,dw\right]^2 \Big/ \left[\int_{-\infty}^{\infty} H_1^2(w)\,dw\right] \tag{39}$$

where w represents an arbitrary coordinate system. In order to place the origin of the z coordinate system, the principal plane of deflection must be known. This is given by:

$$w_P = \left[\int_{-\infty}^{\infty} wH_1(w)\,dw\right] \Big/ \left[\int_{-\infty}^{\infty} H_1(w)\,dw\right]. \tag{40}$$

Now define the z-coordinate system by:

$$z = w - w_P + l_e/2. \tag{41}$$

The image curvature can now be predicted by measuring $H_1(w)$, determining $l_e$ from (39), $w_P$ from (40) and the z-coordinate system from (41). This gives L. To get the image curvature use (34), substituting $l_e$/L for $\lambda$.

Therefore, in order to predict the image curvature, it is necessary to know only $H_1(w)$, the field distribution along the axis.

*The $H_2(z)$ Contributions*

Even though the surface of least confusion, that is the mean image curvature, is independent of $H_2(z)$ in (3), nearly all other properties of the yoke are extremely sensitive to that function. It is, therefore, important to adjust $H_2(z)$ carefully to obtain desired results.

$H_2(z)$ can be used to give anastigmatic yokes, or purposely astigmatic yokes to fulfill special purposes such as line focus, etc. These possibilities will now be taken up in turn. Since for every special purpose $H_2(z)$ will depend very sensitively on $H_1(z)$, it shall be assumed in what follows that $H_1(z)$ is a uniform field of length $l$, where $l << L/3$. Similar calculations, of course, can be made for any particular $H_1(z)$ distribution.

*Anastigmatic Deflection.* An examination of Fig. 6 will show that if it is desired for the beam, converged on the surface of least confusion, to be a point, then $R_T = R_P = R$. In equations (25) this means that $J_T = J_P$. Substituting the assumed constant $H_1$, gives, neglecting terms of the order $(l/L)^2$:

$$H_2 \approx H_1 - (3/2l^2). \tag{42}$$

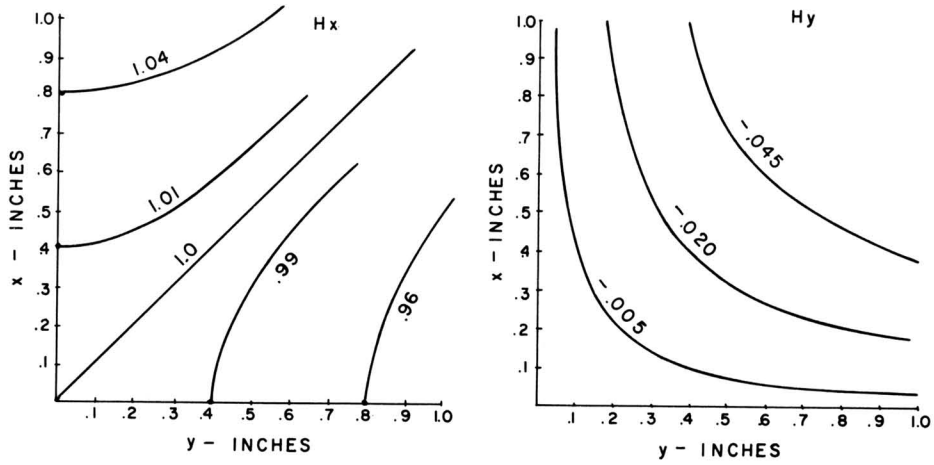


Fig. 10. Example of a non-astigmatic field distribution. ($\ell$ equals 5).

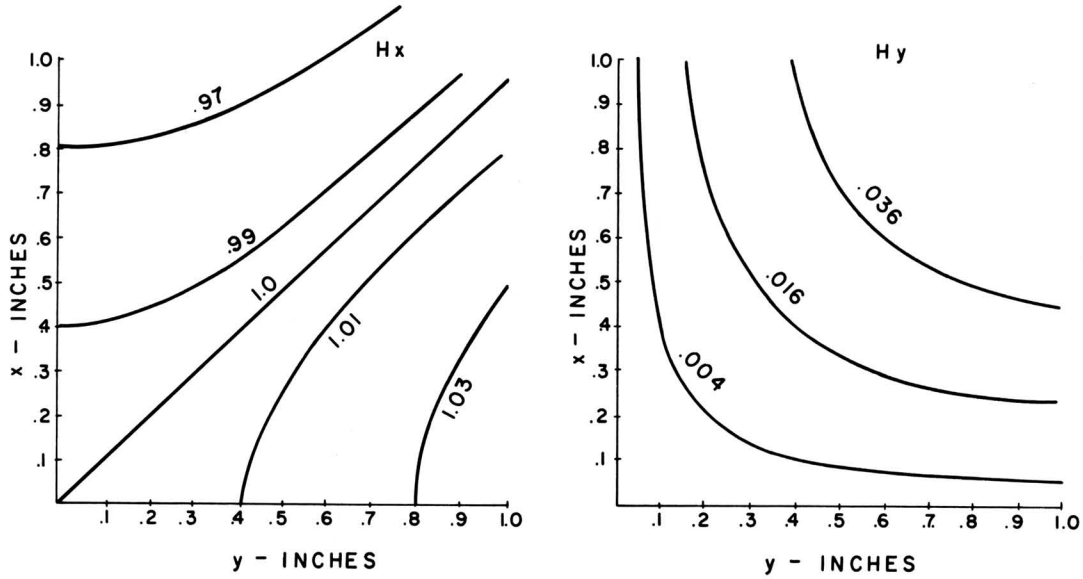


Fig. 11. Vertical deflection field with a horizontal line convergence length, $\ell$, of 5 inches and a field-screen distance, L, of 20 inches.

Recalling (3) and the fact that for the assumed uniform $H_1(z)$ field the derivatives are zero, gives for the deflection field:

$$H_x = H_1\left[1 + (3/2)(x^2/l^2) - (3/2)(y^2/l^2)\right]$$
$$H_y = -3H_1(xy/l^2) \qquad (43)$$
$$H_z = 0.$$

Fig. 10 shows the field distribution for an anastigmatic coil with a length $l$ of about 5 inches.

*Horizontal Line Convergence.* In the case of a line screen, it may be only necessary to converge to a horizontal or vertical line, rather than a round spot. Fig. 6 shows that in that case $R_T = \infty$ or $J_T = 0$. Applying this condition to equations (25) and assuming a uniform $H_1$ as before:

$$H_2 \approx H_1(9/2lL). \qquad (44)$$

Substituting into (3), gives for the field distribution:

$$H_x = H_1\left[1 - (9/2)(x^2/lL) + (9/2)(y^2/lL)\right]$$
$$H_y = 9H_1(xy/lL) \qquad (45)$$
$$H_z = 0.$$

Such a magnetic field would produce a spot converged on a horizontal line. Fig. 11 gives such a field distribution for a yoke screen distance L = 20 and a yoke length $l$ = 5.

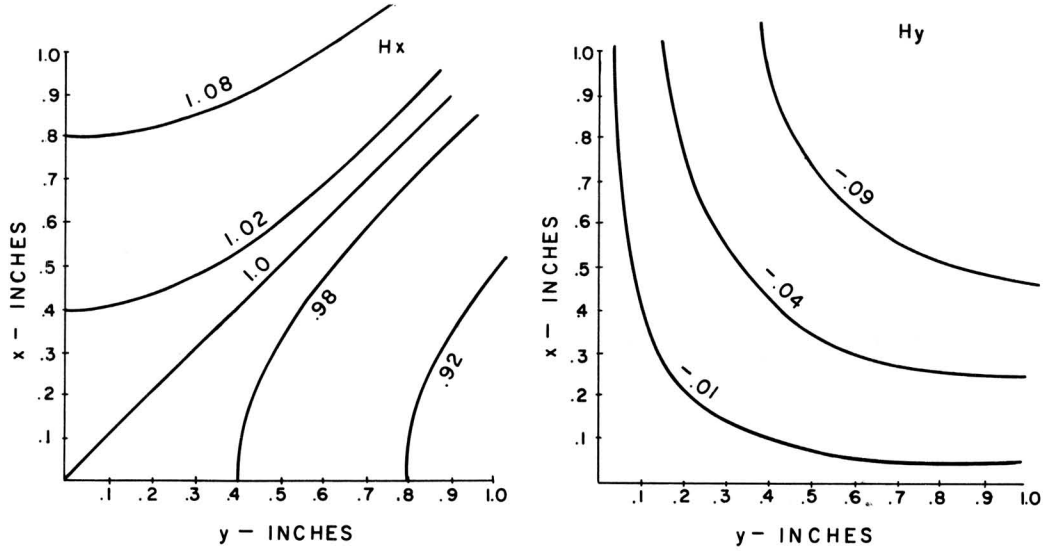


Fig. 12. Vertical deflection field with a vertical line convergence length, $l$, of 5 inches.

*Vertical Line Convergence.* If it is desired to bring about convergence on a vertical line, then Fig. 6 shows that $R_P = \infty$, or $J_P = 0$. (Since all the calculations are for vertical deflection coils, it is obvious that if it is desired to have both vertical and horizontal deflection coils produce horizontal line convergence it is only necessary to rotate the field here calculated through ninety degrees and use it as a horizontal deflection coil).

The condition $J_P = 0$, when applied to (25) with uniform short $H_1(z)$, gives for $H_2$

$$H_2 = - H_1 (3/l^2). \tag{46}$$

Substituting into (3), gives for the field distribution:

$$\begin{aligned} H_x &= H_1 \left[ 1 + 3(x^2/l^2) - 3(y^2/l^2) \right] \\ H_y &= -6H_1 (xy/l^2) \\ H_z &= 0. \end{aligned} \tag{47}$$

Fig. 12 shows such a field distribution for a yoke length $l = 5$.

*Extrapolation to Higher Angles*

The radius of image curvature R implies that the surface of least confusion in the y-z plane is given by

$$y^2 + 2wR + w^2 = 0, \tag{48}$$

where w is given by (z-L). This equation must hold for small angles. On the other hand, for larger angles, the fact that the surface has to pass through y = 0, w = –L can be used. This can be achieved by modifying the $w^2$ term. This gives for the complete surface:

$$y^2 + 2Rw + (2R/L) w^2 = 0. \tag{49}$$

Or in the z-coordinate system:

$$y^2 - 2Rz + (2R/L) z^2 = 0. \tag{50}$$

Equation (50) is easily recognized as an ellipse with the center at y = 0, z = L/2, with a semi-major axis in the z-direction of magnitude L/2, and a semi-minor axis in the y-direction of magnitude $(RL/2)^{1/2}$. Fig. 13 gives such surfaces of best convergence for various values of $l/L = \lambda$.

*Spot Size*

From (16) and (33), the shape of the spot on a flat screen can be evaluated. The spot must be an ellipse with semi-axes given by a and b such that:

$$a + b \approx L(1 + L/l) \alpha \tan^2 \sigma, \tag{51}$$

where $\alpha$ is the aperture angle (r/L) (See Fig. 4) and $\sigma$ is the deflection angle.

The significance of the $H_2(z)$ function is that a and b can be changed at will, as long as the sum a+b remains constant. This result is in essential agreement with E. Gundert.[4]

4. E. Gundert, *Dimensionierung von Kathodenstrahlrohren,* Telefunkenrohre, Heft IV, 1953.

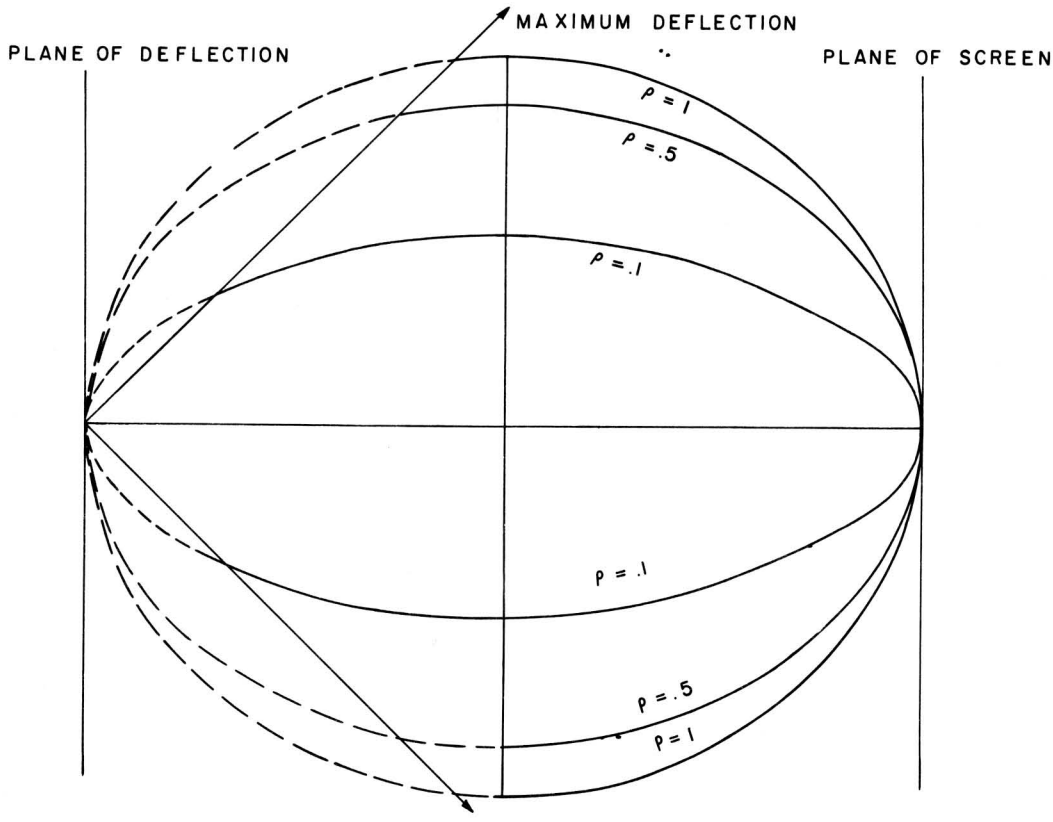


Fig. 13. Surfaces of best convergence for various field lengths ($\rho$ equals $\ell/L$).

## Conclusions

The following conclusions can be drawn from this investigation:

(a). The main features of a deflection field can be obtained by relatively few measurements of the magnetic flux. Due to the symmetry properties of a deflection coil and Maxwell's equations, measurements on the central axis and along one line parellel to the central axis give the field anywhere reasonably close to the axis.

(b). The surface of best convergence bends rather sharply towards the source of electrons. Under the best circumstances, it would have a radius of curvature approximately equal to 0.4 of the distance, gun to screen. Since such a curvature is impractical for a screen, it is necessary to use dynamic focusing. Therefore, it is to be concluded that the effect known as degrouping in shadow mask tubes cannot be eliminated by shaping the magnetic yoke field such that dynamic focusing becomes unnecessary, but must be corrected by other means.

(c). However, in the case of a line screen where it is only necessary to form a vertically converged spot, it is theoretically possible to design a yoke which would give the desired result without the use of dynamic convergence.

(d). Relaxation of the conventional symmetry properties of yokes would make these conclusions invalid. It may be possible to eliminate image curvature for asymmetric yokes. Significant improvements may result from an investigation of this possibility.

Peter E. Kaus

Peter E. Kaus